Accepted Manuscript

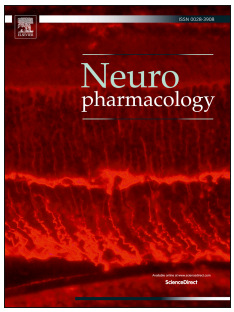

Exploring the Positive Allosteric Modulation of Human α7 Nicotinic Receptors from a Single-Channel Perspective

Natalia D. Andersen, Beatriz E. Nielsen, Jeremías Corradi, María F. Tolosa, Dominik Feuerbach, Hugo R. Arias, Cecilia Bouzat

PII: S0028-3908(16)30067-3

DOI: 10.1016/j.neuropharm.2016.02.032

Reference: NP 6192

To appear in: *Neuropharmacology*

Received Date: 4 September 2015

Revised Date: 20 January 2016

Accepted Date: 24 February 2016

Please cite this article as: Andersen, N.D., Nielsen, B.E., Corradi, J., Tolosa, M.F., Feuerbach, D., Arias, H.R., Bouzat, C., Exploring the Positive Allosteric Modulation of Human α7 Nicotinic Receptors from a Single-Channel Perspective, *Neuropharmacology* (2016), doi: 10.1016/j.neuropharm.2016.02.032.

Exploring the Positive Allosteric Modulation of Human α7 Nicotinic Receptors from a Single-Channel Perspective

Natalia D. Andersen[a], Beatriz E. Nielsen[a], Jeremías Corradi[a], María F. Tolosa[a], Dominik Feuerbach[b], Hugo R. Arias[c], Cecilia Bouzat[a]

[a]Universidad Nacional del Sur/CONICET, Instituto de Investigaciones Bioquímicas de Bahía Blanca, 8000 Bahía Blanca, Argentina.

[b]Neuroscience Research, Novartis Institutes for Biomedical Research, Basel, Switzerland.

[c]Department of Medical Education, California Northstate University College of Medicine, Elk Grove, CA, 95757, USA.

To whom correspondence should be addressed: Cecilia Bouzat, Universidad Nacional del Sur/CONICET, Instituto de Investigaciones Bioquímicas de Bahía Blanca, Camino La Carrindanga Km 7, Bahia Blanca, Argentina. Tel: 54 (291) 4861201; Fax: 54 (291) 4861200; Email: inbouzat@criba.edu.ar

ABSTRACT

Enhancement of α7 nicotinic receptor (nAChR) function by positive allosteric modulators (PAMs) is a promising therapeutic strategy to improve cognitive deficits. PAMs have been classified only on the basis of their macroscopic effects as type I, which only enhance agonist-induced currents, and type II, which also decrease desensitization and reactivate desensitized nAChRs. To decipher the molecular basis underlying these distinct activities, we explored the effects on single-α7 channel currents of representative members of each type and of less characterized compounds. Our results reveal that all PAMs enhance open-channel lifetime and produce episodes of successive openings, thus indicating that both types affect α7 kinetics. Different PAM types show different sensitivity to temperature, suggesting different mechanisms of potentiation. By using a mutant α7 receptor that is insensitive to the prototype type II PAM (PNU-120596), we show that some though not all type I PAMs share the structural determinants of potentiation. Overall, our study provides novel information on α7 potentiation, which is key to the ongoing development of therapeutic compounds.

Keywords: Cys-loop receptors; Nicotinic Receptors; Patch-clamp; Single-channel Recordings; Positive allosteric modulators.

Abbreviations: nAChR, nicotinic acetylcholine receptor; ACh, acetylcholine; 5-HT_3A, serotonin type 3A receptor; PAM, positive allosteric modulator; PAM-2, 3-furan-2-yl-N-p-tolyl-acrylamide; PAM-3, 3-furan-2-yl-N-o-tolylacrylamide, PAM-4, 3-furan-2-yl-N-phenylacrylamide; PNU-120596, *N*-(5-Chloro-2,4-dimethoxyphenyl)-*N*'-(5-methyl-3-isoxazolyl)-urea; 5-HI, 5-Hydroxyindole; NS-1738, *N*-(5-Chloro-2-hydroxyphenyl)-*N*'-[2-chloro-5-(trifluoromethyl)phenyl]urea; RT, room temperature; ECD, extracellular domain, TMD, transmembrane domain; extracellular solution (ECS).

1. INTRODUCTION

α7 nicotinic receptors (nAChRs) are widely distributed in the brain, especially in the hippocampus, thalamus, and cortex (Albuquerque et al., 2009). They contribute to cognition, sensory information processing, attention, working memory, and reward pathways. Decline or alterations of cholinergic signaling involving α7 have been implicated in various neurological diseases, such as schizophrenia, epilepsy, and Alzheimer's disease (Dani and Bertrand, 2007;Dineley et al., 2015;Hurst et al., 2013;Thomsen et al., 2010;Wallace and Bertrand, 2013;Wallace and Porter, 2011). Selective α7 agonists are currently being developed for the treatment of memory impairment in patients with schizophrenia and Alzheimer's disease (Fan et al., 2015;Freedman, 2014;Wallace and Porter, 2011). An alternative approach to increase α7 function is the use of selective positive allosteric modulators (PAMs) (Arias, 2010;Uteshev, 2014;Williams et al., 2011a). Allosteric ligands have several pharmacological advantages over orthosteric ligands including maintenance of the normal spatial and temporal pattern of endogenous neurotransmission and higher receptor subtype selectivity, resulting, at least hypothetically, in high clinical efficacy with minimal adverse effects (Uteshev, 2014).

PAMs have been classified on the basis of their macroscopic effects as type I (e.g., 5-HI, NS-1738) or type II (e.g., PNU-120596). Based on their macroscopic effects it has been postulated that type I PAMs only enhance agonist-induced currents without affecting macroscopic current kinetics, whereas type II PAMs also delay desensitization and reactivate desensitized receptors (Arias, 2010;Bertrand and Gopalakrishnan, 2007;Williams et al., 2011a). The microscopic origin of these profiles remains unclear for most PAMs and its elucidation requires high-resolution single-channel recordings.

We have recently synthesized a series of compounds, named as PAM-2, PAM-3, and PAM-4 and shown that they act as selective α7 PAMs (Arias et al., 2011). Initial Ca^{2+} influx

experiments show that PAM-2 reactivates desensitized α7, suggesting that it is a putative type II PAM (Targowska-Duda et al., 2014). The potential clinical importance of these PAMs is based on experimental results in rodents revealing that PAM-2 produces antidepressant-like (Targowska-Duda et al., 2014;Arias et al., 2015), pro-cognitive (Potasiewicz et al., 2015), and nociceptive and anti-inflammatory activities (Bagdas et al., 2015).

Considering the wide spectrum of potential clinical uses of PAMs, understanding the underlying molecular mechanism of potentiation at human α7 is urgent. Still, studying α7 at the molecular level is complex due to its low open probability and fast kinetics, high-resolution single-channel recordings being therefore required to collect accurate information (Bouzat et al., 2008). We therefore performed a thorough evaluation at the single-channel current level of the activity of prototypic type I and type II PAMs and of the less characterized compounds (PAM-2, -3 and -4). Overall, by examining PAM activities from a different perspective, our results provide novel information regarding the foundation of α7 potentiation, which is required for understanding the potential consequences at the cell and clinical levels.

2. MATERIALS AND METHODS

2.1. Drugs.

5-Hydroxyindole (5-HI), acetylcholine (ACh), and probenecid were purchased from Sigma-Aldrich (St Louis, MO, USA). NS-1738 (*N*-(5-Chloro-2-hydroxyphenyl)-*N*'-[2-chloro-5-(trifluoromethyl)phenyl]urea), PNU-120596 (*N*-(5-Chloro-2,4-dimethoxyphenyl)-*N*'-(5-methyl-3-isoxazolyl)-urea), (±)-epibatidine hydrochloride were obtained from Tocris Biosciences (Bristol, UK). Fluo-4 was purchased from Molecular Probes (Eugene, OR, USA). PAM-2 (3-furan-2-yl-N-p-tolylacrylamide), -3 (3-furan-2-yl-N-o-tolylacrylamide) and -4 (3-furan-2-yl-N-phenylacrylamide) were synthesized as in Arias et al. (2011).

2.2. Expression of Receptors.

All cDNAs were subcloned in the pRBG4 plasmid (Bouzat et al., 1994). Wild-type human α7 (Andersen et al., 2013;Bouzat et al., 2008) and the quintuple mutant α7 (α7TSLMF) that carries five substitutions within the transmembrane domain (TMD) (S223T, A226S, M254L, I281M, and V288F) (daCosta et al., 2011) were used. This quintuple mutant α7 is insensitive to PNU-120596 (daCosta et al., 2011). The chimeric receptor α7-5HT$_3$A is composed of human α7 sequences from the extracellular domain (ECD) and mouse 5-HT$_3$A (m5-HT$_3$A) sequences from the TMD (Bouzat et al., 2004). The high conductance forms of m5-HT$_3$A and the α7-5HT$_3$A chimera were obtained by substitution of three arginine residues responsible for low conductance (R432Q, R436D and R440A) as described before (Corradi et al., 2009;Rayes et al., 2005). BOSC 23 cells, modified HEK 293 cells, were transfected by calcium phosphate precipitation with subunits cDNAs alone or with Ric-3 cDNA to increase α7 cell membrane expression (Andersen et al., 2013;Andersen et al., 2011;Bouzat et al., 2008). Ric-3 and α7 cDNAs were co-transfected at a ratio of 12:1 (wt:wt), with the total α7 cDNA ranging from ~0.4 to 1 µg for a 35-mm culture dish (Andersen et al., 2013;Andersen et al., 2011;Bouzat et al.,

2008). All transfections were carried out for about 12-18 h in DMEM with 10% FBS and were terminated by exchanging the medium. Cells were used for single-channel recordings 2 to 4 days after transfection. To facilitate identification of transfected cells, a separate plasmid encoding green fluorescent protein was included in all transfections.

2.3. Single-Channel Recordings.

Single-channel recordings were obtained in the cell attached patch configuration. For α7 nAChRs, the bath and pipette solutions contained 142 mM KCl, 5.4 mM NaCl, 1.8 mM $CaCl_2$, 1.7 mM $MgCl_2$, and 10 mM HEPES (pH 7.4). For α7-5HT_3A, the bath and pipette solutions contained 142 mM KCl, 5.4 mM NaCl, 0.2 mM $CaCl_2$, and 10 mM HEPES (pH 7.4) (Bouzat et al., 2008). ACh alone and/or PAMs were added to the pipette solution. Single-channel currents were digitized at 5- to 10-μs intervals, low-pass filtered at a cutoff frequency of 10 kHz using an Axopatch 200 B patch-clamp amplifier (Molecular Devices), and analyzed using the program TAC with the Gaussian digital filter at 9 kHz. Gaussian filter of 3 kHz was used in recordings with PNU-120596 to facilitate the analysis. Single-channel currents were detected by the half amplitude threshold criterion using the program TAC (Bruxton Corporation, Seattle, WA, USA). Dwell-time histograms were fitted by the sum of exponential functions by maximum likelihood using the program TACFit (Bruxton Corporation, Seattle, WA, USA).

Bursts of channel openings were identified as a series of closely separated openings preceded and followed by closings longer than a critical duration, which was taken as the point of intersection between the first and second briefest components in the closed-time histogram for bursts of α7 (~300-500 μs), second and third closed components for bursts of α7TSLMF (~1-2 ms), second and third closed components for bursts of α7 in the presence of 5-HI (~1-3 ms), and second and third closed components for bursts of α7-5HT_3A receptors (~2-5 ms) (Andersen et al., 2013). In the presence of PNU-120596, α7 openings are grouped in bursts, which, in turn,

form long clusters. For bursts, the critical time was set at 200-300 μs, and for clusters, the critical time was determined by the point of intersection between the third and fourth closed components (~50 ms).

Single-channel recordings were performed at room temperature (22 ± 2°C) unless specified. To perform recordings at more physiological temperatures we used a thermostated stage and the temperature of the bath solution in the dish was controlled by a thermocouple. The bath temperature was maintained at 34 ± 3°C.

The final concentration of DMSO used to solubilize PAMs was lower than 1% (v/v). As a control, we verified that the mean duration of α7 openings in the presence of ACh and 5 μM PAM-2 does not change if the concentration of DMSO is increased from 0.1% to 1%, discarding the possibility that DMSO is affecting the determined values.

2.4. Macroscopic current recordings.

Currents were recorded in the whole-cell configuration as described previously (Bouzat et al., 2008;Corradi et al., 2009). The pipette solution contained 134 mM KCl, 5 mM EGTA,1 mM $MgCl_2$, and 10 mM HEPES (pH 7.3). The extracellular solution (ECS) contained 150 mM NaCl, 1.8 mM $CaCl_2$, 1 mM $MgCl_2$, and 10 mM HEPES (pH 7.3). Agonist responses (control currents) were obtained by a pulse of ECS containing the agonist.

To study the activity of different PAMs, responses were evaluated following different protocols (Gumilar and Bouzat, 2008). Briefly, we used: co-application protocols, where a 3-s pulse of ECS containing ACh and PAM was applied; pre-incubation protocols, where the cell was exposed to a variable period (6-240 s) to ECS containing PAM before the application of ACh solution; and a combination of both protocols. For all tested PAMs, a 6-s wash period allowed total recovery of control currents. For NS-1738, PNU-120596, PAM-2 and -4 maximal

potentiation was observed with preincubation (with or without co-application). For 5-HI we used co-application assays as reported previously (Zwart et al., 2002).

The solution exchange time was estimated by the open pipette and varied between 0.1 and 1 ms (Corradi et al., 2009). Briefly, an open tip is placed in the ECS stream and the solution is switched to another ½ diluted ECS solution, which leads to a change in liquid junction potential. The time required to produce the 20%-80% change is determined as the exchange time. For the whole-cell configuration the solution exchange rate is slower than that determined for the open pipette because of the larger surface and curvature of the cell compared with the tip. The speed of the solution exchange sensed by the patch in the whole-cell configuration has been estimated to be 3-10-fold slower than that determined from the open pipette (Lovinger et al., 2002;Zhou et al., 1998).

Currents were filtered at 5 kHz, digitized at 20 kHz, and analyzed using the IgorPro software (WaveMetrics Inc., Lake Oswego, OR, USA). Each current represents the average from 3-5 individual traces obtained from the same cell, which were aligned with each other at the point where the currents reached 50% of maximum. Currents were fitted by a double exponential function (1):

$$I(t)=I_{fast}[\exp(-t/\tau_{fast})]+ I_{slow}[\exp(-t/\tau_{slow})]+I_{\infty} \quad (1)$$

where I_{fast} and I_{slow} are the peak current values, I_{∞} the steady state , and τ_{fast} and τ_{slow} are the fast and slow decay time constants, respectively. Net charge was calculated by current integration (Papke and Porter Papke, 2002).

2.5. Ca2+ influx measurements in the GH3-α7 cell line.

The reactivation of desensitized α7 receptors elicited by selective PAMs was determined by Ca^{2+} influx experiments using the GH3-α7 cell line as previously described (Arias et al., 2011). Briefly, $5x10^4$ cells per well were seeded 48 h prior to the Ca^{2+} influx experiment on black poly-L-lysine 96-well plates (Costar, Corning Inc., NY, USA) and incubated at 37°C in a humidified atmosphere (5% CO_2/95% air). On the day of the experiment, the medium was removed by flicking the plates and replaced with 100 µL HBSS/1% FBS containing 2 µM fluo-4 (Molecular Probes, Eugene, OR, USA) in the presence of 2.5 mM probenecid. The cells were then incubated at 37°C in a humidified atmosphere (5% CO_2/95% air) for 1 h. Plates were flicked to remove excess of fluo-4, washed with HBSS/1% FBS, and finally refilled with 100 µL of HBSS. Plates were then placed in the cell plate stage of the fluorimetric imaging plate reader (Molecular Devices, Sunnyvale, CA, USA). 0.1 µM (±)-epibatidine was injected after 8 s, and the fluorescence recorded for a total of 190 s. The laser excitation and emission wavelengths were 488 and 510 nm, at 1 W, with a CCD camera opening of 0.4 s. After nAChR desensitization increasing concentrations of the compound under study were added in the presence of (±)-epibatidine to the cell plate simultaneously to fluorescence recordings for additional 180 s. The concentration–response data for PAM-2, -3, and -4, were curve-fitted by nonlinear least squares analysis using the Prism software (GraphPad Software, San Diego, CA) and the potency (apparent EC_{50} values) and efficacy (E_{max}) of receptor reactivation calculated. ΔE_{max} corresponds to the difference between the maximal fluorescence value (E_{max}) obtained at the highest PAM concentrations and the value obtained after (±)-epibatidine-induced α7 nAChR desensitization.

2.6. Statistics.

Experimental data are shown as mean ± S.D. Student t-Test or One-Way ANOVA were used to determine significance differences. A value of $p<0.05$ was considered statistically significant.

3. RESULTS

3.1. Effects of PAMs on macroscopic currents.

We first determined if the less characterized compounds (PAM-2 and PAM-4) behave at the macroscopic level as type I or type II by analyzing their effects on ACh-activated whole-cell currents from cells expressing human wild-type α7 and comparing with those elicited by prototype PAMs.

In agreement with previous reports (Bertrand and Gopalakrishnan, 2007;Timmermann et al., 2007;Zwart et al., 2002), the type I PAMs 5-HI and NS-1738 increase the amplitude of wild-type α7 whole-cell responses without producing significant changes in the decay time constants (Figure 1). In the presence of 2 mM 5-HI and 50 µM ACh, the maximal current increases 7.7 ± 1.1 times, the net charge increases 5.5 ± 2.3 times, and the decay time constant remains similar to that of the control current. The observed τ_{fast} and τ_{slow} values are 270 ± 130 ms and 1,700 ± 600 ms, and 110 ± 30 ms and 990 ± 40 ms for α7 in the absence and presence of 2 mM 5-HI, respectively (Figure 1). In the presence of 10 µM NS-1738, the peak current increases 2.4 ± 1.1 times, the net charge increases 1.9 ± 1.1 times, and the decay time constants remain unchanged (Figure 1). Thus, the ratio of the changes in net charge/peak current induced by 5-HI and NS-1738 is close to 1, as expected for type I PAMs.

Preincubation with 3 µM PNU-120596 (type II PAM) increases the peak current (23 ±12 times) and produces a significant reduction in the decay rate of wild-type α7 receptors activated

by 50 μM ACh (daCosta et al., 2011) (Figure 1). In general, an initial rapid desensitizing peak current followed by the potentiated current is observed (daCosta et al., 2011;Szabo et al., 2014). The net charge increases 128 ± 100 fold (n=5). Thus, the ratio of the increase in net charge/peak current is >1, in accordance to previous observations (Williams et al., 2011b). At a saturating ACh concentration (1 mM), α7 potentiation by PNU-120596 is also important but it is slightly smaller than that at 50 μM ACh (peak current and net charge increase 23 ± 18 and 61 ± 28 fold respectively, n=9) (Figure S1).

Preincubation with 100 μM PAM-2 or PAM-4 enhances the peak current and decreases the decay rate of wild-type α7 ACh-evoked currents (Figure 1). Higher PAM concentrations (300 and 500 μM) do not produce further potentiation. PAM-2 and PAM-4 increase 1.5 ± 0.2 and 1.8 ± 0.5 times the peak of ACh-elicited currents, and 4.2 ± 0.1 and 3.7 ± 2.4 times the net charge, respectively. The decreased decay rate together with the fact that the ratio of the change in net charge versus the change in peak current is > 1 supports a type II classification, as previously suggested for PAM-2 (Targowska-Duda et al., 2014).

α7 potentiation by PAM-2 is smaller at 1 mM ACh than at 50 μM ACh (the peak current decreases 0.6 ± 0.2 fold and the net charge increases only 2.1 ± 0.8 fold, n=4) (Figure S1). This weak potency make PAM-2 appear under certain conditions as an intermediate type PAM.

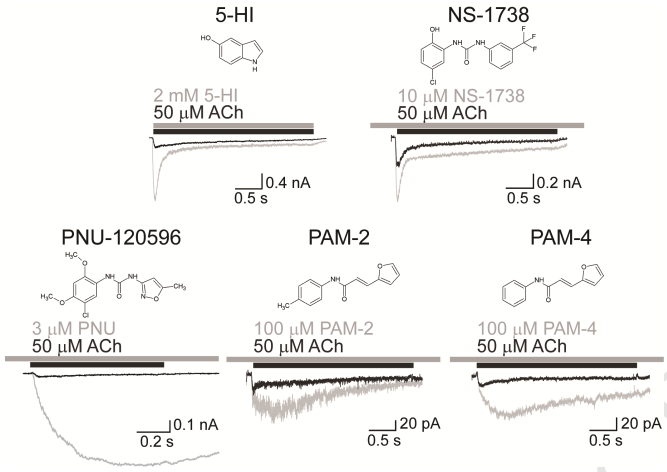

FIGURE 1. Potentiation of wild-type α7 responses by type I and type II PAMs. Whole-cell α7 currents elicited by 50 μM ACh (black traces), and 50 μM ACh plus a given PAM (grey traces), including 5-HI (n=3), NS-1738 (n=9), PNU-120596 (n=5), PAM-2 (n=10), and PAM-4 (n=9). The bars show the application of ACh (black) and PAM (grey). Membrane potential: -50 mV.

3.2. Reactivation of desensitized α7 nAChRs by selective PAMs.

Ca^{2+} influx assays were performed in GH3-α7 cells to quantitatively compare the activity of PAM-2, -3 and -4 with that of NS-1738 and PNU-120596 (Figure 2A). After the initial (±)-epibatidine-induced α7 activation (i.e., increased Ca^{2+} influx), receptors become desensitized. The subsequent treatment of cells with either PAM-3, PAM-4, or PNU-120596 in the presence of (±)-epibatidine reactivates the formerly desensitized α7, and a long-lasting Ca^{2+} increase is observed (Figure 2A). These results are in agreement with that described initially for PAM-2 (Targowska-Duda et al., 2014). In contrast, NS-1738 does not produce reactivation (Figure 2A), thus confirming that PAM-2, -3, and -4, can be considered type II PAMs. To quantify the reactivation induced by PAM-2, -3, -4 and PNU-120596, increasing concentrations of each PAM were used (Figure 2B). The results indicate that PAM-2 and -4 are equipotent and ~3-fold more

potent than PAM-3, and that PNU-120596 is the most potent among all tested PAMs (Table 1). This trend coincides very well with the potencies determined previously (Arias et al., 2011). The ΔE_{max} values indicate the following efficacy order: PNU-120596>PAM-2~PAM-4>PAM-3 (Table 1).

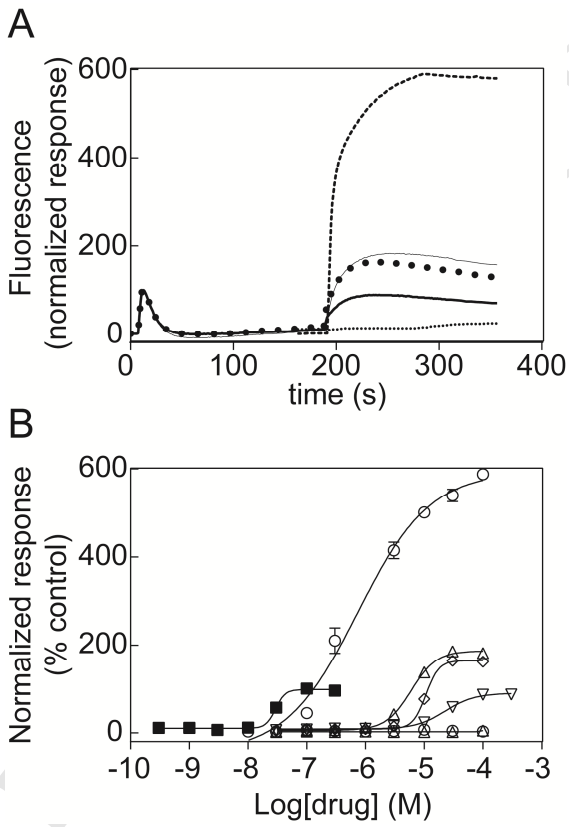

FIGURE 2. Reactivation of desensitized α7 by selective PAMs.

(A) GH3-α7 cells were first treated with 0.1 μM (±)-epibatidine. After desensitization, cells were treated with either 10 μM PAM-2 (─), -3 (▬), -4 (•••), PNU-120596 (---), or NS-1738 (…) in the presence of 0.1 μM (±)-epibatidine. (B) To quantify the reactivation activity of PAMs, increasing concentrations of PAM-2 (△), -3 (▽),-4 (◊), PNU-120596 (○), and NS-1738 (□) were used. The observed plots are representative of 3 experiments. (±)-Epibatidine-induced α7 nAChR activation (■) is also included for comparative purposes. The data for PAM-2 was taken from Targowska-Duda et al. (2014) for comparative purposes.

TABLE 1. Potency (EC_{50}) and differential efficacy (ΔE_{max}) of PAMs for recovering desensitized α7 nAChRs from GH3 cell line.

PAM	Apparent EC_{50} (μM)	ΔE_{max}
PAM-2	3.6 ± 1.8	183 ± 65
PAM-3	14.9 ± 7.1	87 ± 15
PAM-4	5.4 ± 3.4	164 ± 38
PNU-120596	0.8 ± 0.5	589 ± 13
NS-1738	No effect	—

The concentration–response data for the different PAMs were analyzed by nonlinear regression (Figure 2B). The ΔE_{max} values correspond to the difference between the E_{max} value obtained at the highest PAM concentrations and the value obtained after (±)-epibatidine-induced α7 nAChR desensitization.

3.3. Single-channel current profiles of wild-type α7 nAChRs potentiated by type I and II PAMs.

To compare the molecular effects elicited by different PAMs, single-α7 channel currents were recorded in the absence and presence of type I (5-HI and NS-1738), type II (PNU-120596), and PAM-2, -3 and -4 compounds. In the absence of modulators, 50-100 μM ACh elicits brief and isolated channel openings from cells expressing α7. The open time distribution is described by a brief exponential component of 60 ± 10 μs and the slowest one of about 300 μs (Figure 3A, Table 2) (Andersen et al., 2013;Bouzat et al., 2008). In the presence of 2 mM 5-HI, single-channel recordings show prolonged α7 openings and bursts composed of successive openings appear (Andersen et al., 2013) (Figure 3B, Table 2). The open-time histogram is fitted by the sum of two or three exponential components, being the mean duration of slowest component

~6-fold longer than that of the control (Table 2). The maximal open-channel lifetime is relatively constant at a range of 5-HI concentration from 100 μM (1.4 ± 0.3 ms) to 2 mM. The mean burst duration is 10-fold longer than that in the absence of PAMs (Figure 3, Table 2). In the presence of 10 μM NS-1738, α7 openings elicited by 100 μM ACh are also prolonged and appear in bursts, similar to the activity observed with 5-HI. Open duration histograms are described by the sum of three exponential components (Figure 3C). The mean durations of the slowest open component and of bursts are statistically significantly longer with respect to those determined in its absence (Figure 3C, Table 2). In conclusion, two representative type I PAMs prolong open duration and make openings appear in long activation episodes, indicating that type I PAMs do affect activation kinetics.

PNU-120596 (1 μM) gives rise to significantly prolonged openings, grouped in bursts of openings separated by brief closings (200-300 μs), which in turn coalesce into long activation periods, named clusters (Table 2 and daCosta et al., 2011). The mean duration of the slowest open component is ~700-fold longer than that in the absence of PAMs (Figure 3D, Table 2).

In the presence of PAM-2 (5 μM), PAM-3 (25 μM), or PAM-4 (5 μM) at concentrations corresponding to their EC_{50} values determined by Ca^{2+} influx assays (Arias et al., 2011), 50-100 μM ACh elicits prolonged openings which are grouped in bursts of ~10 ms (Figure 3E-G and Figure S2, Table 2). For the three PAMs, open duration histograms are fitted by three exponential components, whose durations are ~0.10 ms, ~0.50-0.70 ms and ~3 ms (Figure 3, Table 2 and Figure S2). For all PAMs, the mean open and burst durations determined at concentrations 3-4 times higher than the corresponding EC_{50} do not show further increase (except for the burst duration between 5 and 20 μM PAM-4) (Figure S2). At lower concentrations (0.1-1 μM PAM-2) openings and bursts are less frequent and significantly briefer than at 5 μM (Figure S2).

In conclusion, the two types of PAMs enhance open and burst durations. Moreover, the single-channel profiles in the presence of PAM-2, -3 and -4 (classified as type II PAMs) resemble better that of type I PAMs than that of PNU-120596 (Figures 1 and 3, Table 2).

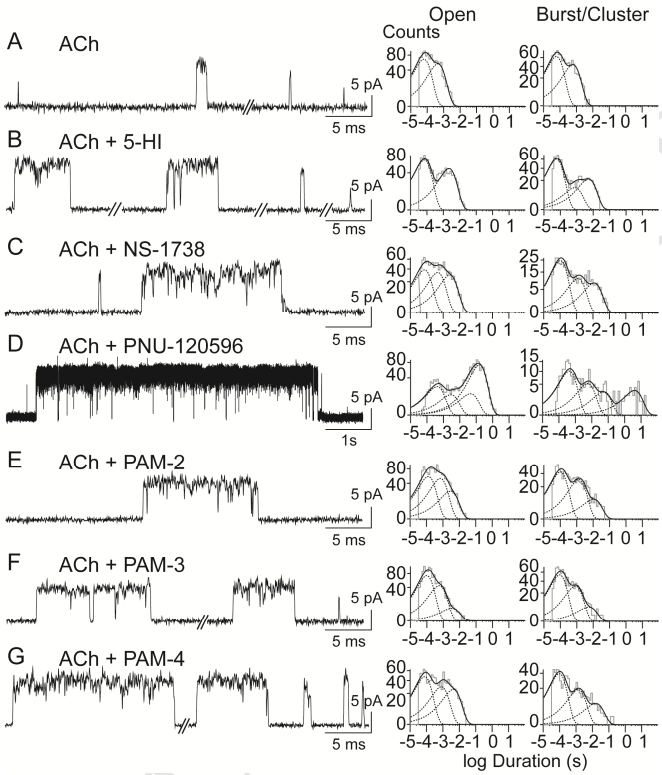

FIGURE 3. Single-channel current profiles of wild-type α7 in the presence of type I and type II PAMs.

Left: Single-channel traces of 50-100 μM ACh-activated α7 currents in the absence of PAMs (**A**), or in the presence of 2 mM 5-HI **(B)**, 10 μM NS-1738 **(C)**, 1 μM PNU-120596 **(D)**, 5 μM PAM-2 **(E)**, 25 μM PAM-3 **(F),** and 5 μM PAM-4 **(G)**. Membrane potential: -70 mV. **Right:** Representative open and burst or cluster duration histograms are shown for each condition.

Table 2. Mean open and burst or cluster durations of α7, 5-HT$_3$A, α7-5HT$_3$A and α7TSLMF in the presence of PAMs.

Receptor	Agonist	Agonist (μM)	PAM	τ_o (ms)	τ_{burst} or $\tau_{cluster}$ (ms)	n
α7	ACh	50-100	-	0.33 ± 0.12	0.43 ± 0.15	6
α7	ACh	100	2 mM 5-HI	2.0 ± 0.6 (***)	4.2 ± 1.9 (*)	8
α7	ACh	100	10 μM NS-1738	2.8 ± 0.6 (***)	12.7 ± 5.9 (**)	4
α7	ACh	100	1 μM PNU-120596	206 ± 79 (***)	2700 ± 1200 (***)	8
α7	ACh	50-100	5 μM PAM-2	2.7 ± 0.9 (***)	9.5 ± 2.9 (***)	8
α7	ACh	50-100	25 μM PAM-3	2.6 ± 0.7 (**)	6.9 ± 1.7 (**)	3
α7	ACh	50-100	5 μM PAM-4	3.5 ± 0.7 (***)	13.2 ± 2.7 (***)	4
5-HT$_3$A	5-HT	1	-	120 ± 35	3200 ± 1300	4
5-HT$_3$A	5-HT	1	5 μM PAM-2	115 ± 50	2600 ± 700	6
5-HT$_3$A	5-HT	1	15 μM PAM-2	60 ± 15 (*)	800 ± 250 (**)	3
α7-5HT$_3$A	ACh	1000	-	9.6 ± 2.8	17.9 ± 6.9	5
α7-5HT$_3$A	ACh	1000	5 μM PAM-2	9.8 ± 2.2	21.3 ± 6.7	6
α7-5HT$_3$A	ACh	1000	2 mM 5-HI	14.2 ± 4.0	73.5 ± 23.4 (**)	3
α7TSLMF	ACh	100	-	1.0 ± 0.4	2.0 ± 1.0	9
α7TSLMF	ACh	100	2 mM 5-HI	5.8 ± 0.9 (***)	22.3 ± 3.7 (***)	4
α7TSLMF	ACh	100	10 μM NS-1738	1.1 ± 0.1	1.5 ± 0.6	4
α7TSLMF	ACh	100	5 μM PAM-2	1.3 ± 0.7	2.5 ± 1.4	7

Single-channel properties of different receptors in the absence and presence of PAMs. τo and τburst or τcluster correspond to the slowest components of the open and burst or cluster duration histograms, respectively. Values are mean ± SD. n: corresponds to the number of patches from different experiments. Statistical significance was determined by comparing the mean value in the presence of the indicated PAM with respect to that determined in its absence (Student t-Test: $p<0.05$ *, $p<0.01$ **, $p<0.001$ ***).

3.4. Temperature dependence of PAM potentiation.

Although most *in vitro* studies have been performed at room temperature (RT), preclinical studies and clinical use obviously take place at physiological temperatures. At the macroscopic level, it has been shown that wild-type α7 currents potentiated by PAMs are markedly reduced if the temperature is increased (Sitzia et al., 2011;Williams et al., 2012). To understand the origin of this effect, we evaluated at the single-channel level PAM potentiation at a temperature closer to the physiological one (34 ± 3℃). As expected, t he single-channel amplitude, measured in the presence of PAMs, is higher at 34°C than that at RT (22 ± 2℃) (Figure 4). The Q_{10} value for single-channel conductance, estimated with these two points, is 1.2. This value is in close agreement with the Q_{10} for the muscle nAChR and indicates that the temperature sensitivity is similar to that of diffusion of ions in solution (Dilger et al., 1991).

Single-channel activity in the presence of PNU-120596 reveals reduced potentiation at 34°C with respect to RT. The mean duration of the slowest open component is reduced 2-fold respect to that at 22°C (Table 3). However, the most important change occurs in the pattern of channel activity. More specifically, bursts do not coalesce into the long clusters observed at RT; they instead appear isolated, thus leading to significantly shorter activation episodes when compared to the 3-s ones detected at RT (Figure 4A). To quantify the kinetic changes we analyzed burst (defined by successive openings separated by closings of durations <0.2 ms) and cluster duration histograms. The mean burst duration is 258 ± 118 ms at 22℃ and 164 ± 40 ms at 34℃. We determined that at 34ºC the mean dur ation of bursts remains constant (206 ± 70 ms, n=5, p>0.05) if the critical time used to define a burst is increased 20-fold (4-5 ms), which corresponds to the intersection between the 2nd and 3rd exponential components of the closed time histograms. The 3rd and 4th closed components are highly variable among recordings at 34°C, suggesting that they correspond to dwell times between independent activation episodes. Therefore, at this temperature, we cannot define activation episodes of

longer duration than a burst, in good agreement with the visual inspection of the recordings (Figure 4). In contrast, for recordings at 22ºC in the presence of PNU-120596, the duration of the 3rd closed component is relatively constant among recordings, and setting the critical time to that corresponding to the intersection of the 3rd and 4th closed components allows definition of the ~3-s clusters (composed of several bursts), which are clearly observed in the recordings. Thus, in the presence of PNU-120596, although the increase in temperature decreases slightly the open-channel lifetime, it decreases markedly the capability of eliciting super long-activation episodes (Figure 4A, Table 3).

We subsequently evaluated the temperature dependence of 5-HI potentiation. Interestingly, visual inspection of recordings at 34ºC shows the presence of the typical bursts of openings but occurring at lower frequency compared to RT (Figure 4B, Table 3). To detect these low-frequency potentiated bursts, open and burst duration histograms were fitted including an additional exponential component. To standardize the analysis, the same procedure was applied to recordings at RT. We found that the slowest exponential components of both histograms, which correspond to the maximal open and burst durations, do not show statistically significant differences between RT and 34ºC (Table 3). This result confirms that for 5-HI the maximal open-channel lifetime at 22ºC can be achieved at 34ºC. Thus, while a higher temperature evokes a marked reduction in the duration of PNU-120596-induced clusters, it does not affect the maximal duration of 5-HI prolonged bursts. Nevertheless, for 5-HI the proportion of potentiated bursts at 34ºC decreases statistically significantly with respect to that at 22^{o}C (relative areas are 0.02 ± 0.01 and 0.05 ± 0.01, respectively, $p<0.05$). Therefore, the overall potentiation would be also reduced at physiological temperatures.

The mean open and burst durations of α7 in the presence of PAM-2 are significantly reduced at 34ºC respect to RT ($p<0.01$) (Figure 4C, Table 3). Although PAM-2 behaves as a type II PAM, the burst duration in its presence is more similar to that in the presence of 5-HI

than in the presence of PNU-120596. We therefore evaluated if fitting burst duration histograms at 34^{o}C with an additional exponential component reveals bursts of mean duration similar to those at 22ºC, as shown for 5-HI. We found no statistically significant differences of mean burst durations calculated from histograms fitted either by four or by three components, thus confirming that the prolonged bursts do not occur at higher temperatures. Overall, the reduction in the duration of sustained activation episodes, which are the most sensitive parameters to temperature, appears to be different among different PAM types.

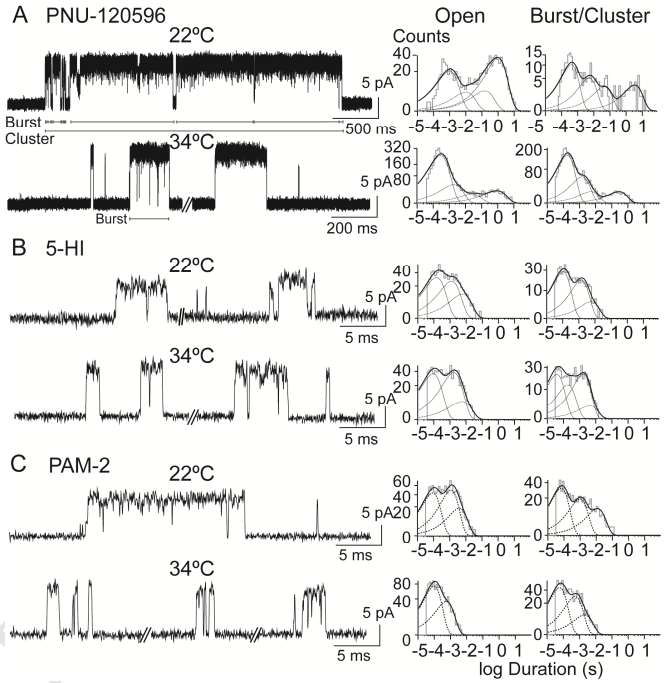

FIGURE 4. Effect of temperature on PAM-induced potentiation of human wild-type α7 single-channel currents.

Left: Single-channel traces of α7 recorded at room temperature (22 ± 2℃) or near physiological temperature (34 ± 3℃) in the presenc e of 50-100 μM ACh and 1 μM PNU-120596 (A), 2 mM 5-HI (B) or 20 μM PAM-2 (C). Membrane potential: -70 mV. Right: Open and burst/cluster duration histograms for each condition are shown.

Table 3. Effect of temperature on α7 PAM potentiation.

Temperature (℃)	ACh (μM)	PAM	τ_o (ms)	τ_{burst} or $\tau_{cluster}$ (ms)	n
22 ± 2	100	1 μM PNU-120596	206 ± 79	2700 ± 1200	8
34 ± 3	100	1 μM PNU-120596	122 ± 37 (*)	206 ± 70(***)	5
22 ± 2	100	2 mM 5-HI	2.4 ± 1.0	4.0 ± 1.3	5
34 ± 3	100	2 mM 5-HI	1.9 ± 0.2	4.1 ± 0.1	4
22 ± 2	50	20 μM PAM-2	3.2 ±0.20	9.9 ± 2.9	3
34 ± 2	50	20 μM PAM-2	1.9 ± 0.4 (**)	2.9 ± 0.6 (**)	3

Single-channel properties of potentiated α7 channels at RT (22 ± 2 ºC) or at more physiological temperatures (34 ± 3 ℃). τ_o and τ_{burst} or $\tau_{cluster}$ correspond to the slowest components of the open and burst or cluster duration histograms, respectively. Values are mean ± SD. n: corresponds to the number of patches from different experiments. Statistical significance was determined by comparing the mean values at the two different temperatures (Student t-Test: $p<0.05$ *, $p<0.01$ **, $p<0.001$ ***).

3.5. 5-HT$_3$A and α7-5HT$_3$A chimeric receptors are not potentiated by PAM-2.

To provide further information on receptor selectivity of PAM-2 (Arias et al., 2011), we explored its action on 5-HT$_3$A and chimeric α7-5HT$_3$A receptors. In the presence of 1 μM 5-HT, single-channel currents are readily detected in cell-attached patches from cells expressing the high-conductance form of 5-HT$_3$A receptors (Figure 5B) (Bouzat et al., 2008;Corradi et al., 2009). Single-channel activity, which in the absence of PAM-2 appears mainly as long openings forming bursts that coalesce in long-lasting clusters, remains constant in the presence of 5 μM PAM-2 (Figure 5B, Table 2). A higher PAM-2 concentration (15 μM) does not lead to further potentiation but reduces open and cluster durations, probably due to open-channel blockade (Figure 5, Table 2). Thus, we conclude that 5-HT$_3$A receptor is not potentiated by PAM-2.

Recordings from cells expressing the α7-5HT$_3$A chimera (Bouzat et al., 2004) show that the mean open and burst durations in the presence of PAM-2 are similar to those in its absence (Figure 5C, Table 2), indicating that PAM-2 is not a positive modulator of α7-5HT$_3$A receptors. In contrast, 5-HI potentiates 5-HT$_3$A receptors (Hu and Lovinger, 2008) and the α7-5HT$_3$A chimera as evidenced by the increased burst duration in its presence (Table 2).

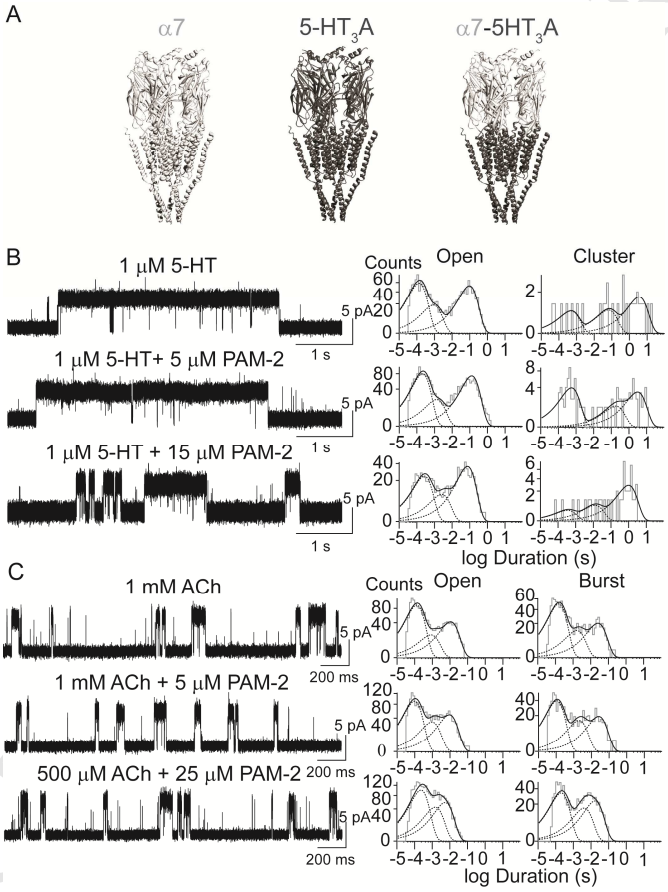

FIGURE 5. Lack of potentiation of 5-HT$_3$A and α7-5HT$_3$A receptors by PAM-2.

(A) Models of the α7, 5-HT$_3$A, and chimeric α7-5HT$_3$A receptors (PDB:2BG9). Protein regions with α7 sequence are shown in light grey, and those with 5-HT$_3$A sequence in dark grey. Single-channel currents from 5-HT$_3$A receptors evoked by 5-HT **(B)** or from α7-5HT$_3$A receptors evoked by ACh **(C),** in the absence or presence of different concentrations of PAM-2. Representative open and burst/cluster duration histograms are shown.

3.6. Structural determinants of α7 potentiation by type I and type II PAMs.

A fundamental question is whether there is a common or different binding site(s) for type I and type II PAMs. We took advantage of our previously reported mutant α7 receptor (α7TSLMF) (daCosta et al., 2011), which carries five mutations at an intrasubunit cavity forming the PNU-120596 binding site (Young et al., 2008), to explore whether all PAMs share the same structural components. Single-channel currents of ACh-elicited α7TSLMF reveal lack of potentiation by PNU-120596 (daCosta et al., 2011) and PAM-2 (Figure 6, Table 2), indicating that PAM-2 and PNU-120596 share the same structural determinants for their potentiating effects, probably as a result of an overlapping binding site. In contrast, the quintuple mutant α7TSLMF activated by 100 μM ACh is potentiated by 2 mM 5-HI in a similar way as wild-type α7 (Table 2). Interestingly, 10 μM NS-1738 does not enhance open channel lifetime and does not produce bursts of openings of α7TSLMF as observed for α7 wild-type (Figure 6, Table 2), indicating that it shares with the type II PAMs the structural determinants required for potentiation.

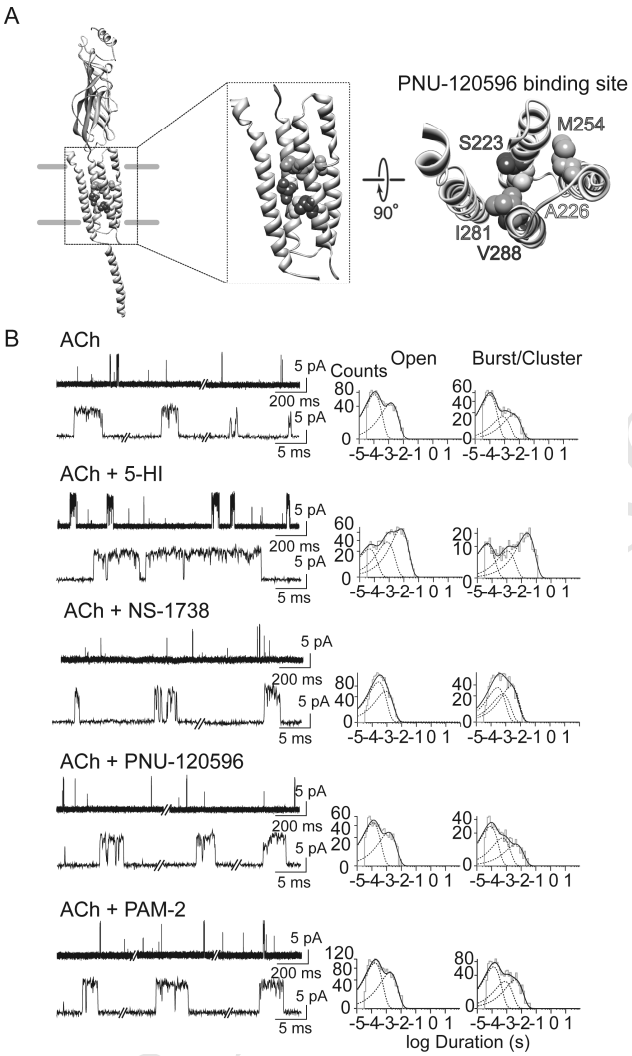

FIGURE 6. Differential potentiation of the human α7 quintuple mutant nAChR (α7TSLMF) by type I and type II PAMs.

(A) Homology model of a single α7 subunit based on the *Torpedo* nAChR structure (PDB 2BG9). Magnified close-up view of the transmembrane region (lateral and top view), highlighting the residues involved in PNU-120596 binding. **(B) Left:** Single-channel traces from α7TSLMF activated by 100 μM ACh in the absence or presence of either 2 mM 5-HI, 10 μM NS-1738, 1 μM PNU, or 5 μM PAM-2. **Right:** Representative open and burst or cluster duration histograms for each condition.

4. DISCUSSION

Since stimulation of neuronal α7 nAChRs improves attention, cognitive performance and neuronal resistance to injury as well as it produces robust analgesic and anti-inflammatory effects, this nAChR has emerged as a potential drug target (Dineley et al., 2015;Thomsen et al., 2011). When compared to agonists, PAMs are promising therapeutic tools because: i) they maintain the temporal spatial characteristics of endogenous activation; ii) they show higher selectivity (Yang et al., 2012); iii) they reduce tolerance due to α7 desensitization; and iv) they act as neuronal protectors (Kalappa et al., 2013;Sun et al., 2013;Uteshev, 2014). Since drug discovery in this field is still in progress, deciphering the molecular mechanism(s) underlying PAM activities at human α7 is urgent. In addition, the characterization of novel PAMs will provide new avenues for therapy. In particular, preclinical studies in rodents have shown potential clinical benefits of PAM-2 compound (Bagdas et al., 2015;Potasiewicz et al., 2015;Targowska-Duda et al., 2014). We here determined that its high selectivity for human α7 together with its moderate potentiation at physiological temperatures make this compound good candidate for clinical use.

α7 activation is unique because: i) ACh occupancy of only one of its five ACh binding sites allows activation and maximal open-channel lifetime, ii) the temporal pattern of single-channel currents is not dependent on agonist concentration, and iii) desensitization rate is so rapid that it is a major determinant of open channel lifetime (Bouzat et al., 2008). Thus, α7 behaves as high fidelity sensor of ACh concentration and harbors a built-in filtering mechanism against excessive stimulation. Any slight changes in the energy barriers between active, closed and/or desensitized states would, therefore, have a deep impact on this unique activation mechanism, thus making these receptors very sensitive drug targets.

Our results indicate that the macroscopic profile of PAM-2-induced α7 potentiation resembles that of type II PAM potentiation as evidenced by the marked decrease in the current decay rate

and the ratio in the net charge/peak current changes. In addition, our Ca^{2+} influx results indicate that PAM-2, -3, and -4 reactivate desensitized α7, which support a type II PAM classification. However, at a saturating ACh concentration potentiation of the macroscopic response is significantly smaller than at submaximal ACh concentration, which may make PAM-2 appear as an intermediate class under certain conditions.

A few number of studies have described the single-channel effects of α7 PAMs, which were limited to the type II PAMs PNU-120596 (daCosta and Sine, 2013;daCosta et al., 2011;Hurst et al., 2005;Williams et al., 2011b) and TQS (Palczynska et al., 2012). In spite of minor quantitative differences likely due to differences in experimental conditions, there is a general consensus that type II PAMs increase the open-channel duration, the number of detectable open states, the burst/cluster duration and the open probability (Andersen et al., 2013;daCosta et al., 2015;daCosta et al., 2011;Hurst et al., 2005;Palczynska et al., 2012;Williams et al., 2011b). There is no full agreement on whether or not there is a change in single-channel conductance. All studies report amplitude distributions showing multiple amplitude populations in the absence of PAMs and a major single population in their presence, which in turn, corresponds to the highest detected amplitude. However, they differ in the interpretation of these observations since lack of full-amplitude resolution due to the brief open durations in the absence of PAMs (Andersen et al., 2013;daCosta et al., 2015;daCosta et al., 2011;Williams et al., 2011b;Yan et al., 2015) and genuine increased conductance have been proposed (Palczynska et al., 2012).

It is a generally accepted statement that type II PAMs may increase the energetic barrier for desensitization and/or reverse some forms of desensitization induced by agonist (Williams et al., 2011a). An increase in the desensitization barrier would lead to a more stabilized open state, which agrees with the observed effects of PNU-120596 and PAM-2 on both macroscopic and single-channel currents. It has also been proposed that PNU-120596 binds predominantly to the fast desensitized state and induces a set of conformational states in which opening of the pore

is energetically more favorable (Szabo et al., 2014). This mechanism explains very well the long openings and activation episodes detected at the single-channel level.

In contrast, and also based on macroscopic observations, it has been postulated that type I PAMs increase the peak of ACh-elicited macroscopic currents without changing the kinetics due to a decrease in the energetic barrier for opening (Hurst et al., 2013;Williams et al., 2011a). Our single-channel data demonstrate that two prototypic type I PAMs increase α7 open-channel lifetime, which reveals that they do affect α7 kinetics. The decrease in the energetic barrier for opening might explain the appearance of bursts of openings observed with type I PAMs due to rapidly re-opening of the closed channel. However, it would only explain the increase in the duration of the open channel if reopening of the closed channel were so fast that the associated brief closings could not be detected, thus making openings appear artifactually longer. Alternatively, same as type II PAMs, the increase in the duration of channel openings in the presence of type I PAMs could be due to changes in desensitization rate, which in turn, could be too slight to be detected from whole-cell macroscopic currents. However, this may not be the case since, although PAM-2 and 5-HI (or NS-1738) produce a similar increase in open and burst durations, the effects on the decay of macroscopic currents are different. Thus, there seems to be more than one mechanism by which PAMs enhance the duration of the open channel and of activation episodes. It is also important to remark that given the fast kinetics of α7, the temporal resolution of the system, including the patch configuration and the perfusion speed, should be taken into account for defining PAM actions. In slow systems, the changes in current decay rates do not strictly correlate with changes in desensitization rates (Bouzat et al., 2008;Lovinger et al., 2002;Zhou et al., 1998). In this regard, we expect that fast outside-out patches should reveal decreased decay rates in the presence of type I PAMs because of the more prolonged openings.

PAMs with intermediate type I/type II properties have been reported (Chatzidaki et al., 2015;Dinklo et al., 2011;Dunlop et al., 2009;Malysz et al., 2009;Sahdeo et al., 2014). As previously suggested (Chatzidaki and Millar, 2015), it could be possible that the classification of type I and type II PAMs is an oversimplification resulting mainly from macroscopic observations. In agreement with this, we here reveal that potentiation is more complex than what it appears to be, i.e. PAM-2 behaves at the macroscopic level as a type II PAM as judged from its effects on the decay rate and its capability of reactivating desensitized receptors. However, its activity at the single-channel level resembles more that of type I PAMs, and at a saturating ACh concentration, the macroscopic effect is very slight. Moreover, NS-1738 macroscopically behaves as a type I PAM but shares structural determinants with type II PAMs.

Macroscopic current studies have shown that α7 potentiation decreases significantly at temperatures closer to physiological values compared to that at RT (Sitzia et al., 2011;Williams et al., 2012). This is indeed an important issue because clinical effects occur at physiological temperatures. In addition, there are controversial results regarding the cytotoxic effects of PNU-120596 due to the profound α7-induced calcium influx (Guerra-Alvarez et al., 2015;Hu et al., 2009;Ng et al., 2007;Uteshev, 2015;Williams et al., 2012). The fact that PAM-induced potentiation is reduced at physiological temperatures may be beneficial in attenuating potential toxicity.

Our temperature dependence results reveal for the first time the microscopic changes underlying the temperature sensitivity of PAM-potentiation. Although there is an important decrease in the duration and/or frequency of long activation episodes between 22^{o}C and 34^{o}C, potentiation is still significant when compared to single-channel activity in the absence of PAMs, which, in turn, support their potential clinical effects. In the presence of PNU-120596, the long clusters observed at RT are absent at physiological temperatures and activation episodes take place in shorter bursts. We show that the longest bursts elicited by PAM-2 also disappear at

higher temperatures. This is different from what is observed for 5-HI, for which maximal open and burst durations can be achieved at physiological temperatures, albeit at a lower frequency than at RT. Thus, this detailed analysis shows differences in the effect of temperature on potentiation between different PAMs. Previous studies have demonstrated that α7 desensitization rate increases at higher temperatures in the absence or presence of PNU-120596 (Gupta and Auerbach, 2011;Jindrichova et al., 2012;Sitzia et al., 2011). If the effect of temperature were mainly on desensitization, increasing temperature would affect mainly type II PAM modulation. This could explain why we observe a reduction in the duration of the longest bursts or clusters in the presence of type II PAMs, while the maximal duration of the bursts with 5-HI remains more constant. These differences suggest that bursts/clusters have a different mechanistic origin in type I (5-HI) or type II PAMs. Nonetheless, more PAMs should be tested to confirm this hypothesis. Alternatively, it could be possible that dissociation of PAMs from their binding sites responds differently to temperature depending on both the PAM and the binding-site structures.

Previous studies using chimeras and point mutations pointed out that type I and II PAMs may bind to a common or overlapping transmembrane site (Collins et al., 2011;Gill et al., 2011;Young et al., 2008). Other studies suggested distinct regions as responsible for the effects elicited by type I or type II PAMs (Bertrand et al., 2008). A similar controversial situation is observed for 5-HI, where both extracellular (Gronlien et al., 2010) and transmembrane site locations have been proposed (Hu and Lovinger, 2008;Placzek et al., 2004). Given the structural diversity of α7 PAM chemotypes, it is likely that there are multiple allosteric sites on the receptor and a given PAM could bind to more than one. In agreement with this, several ECD sites have been proposed for type I PAMs (Spurny et al., 2015).

Our results showing that neither PAM-2 nor PNU-120596 potentiates α7TSLMF support that these two PAMs share similar structural determinants and probably an overlapping site. In

support of this conclusion, both PAMs produce qualitatively similar effects at both the macroscopic and single-channel levels and respond similarly to the increased temperature. Interestingly, whereas NS-1738 behaves more similar to 5-HI, it shares the structural determinants of PNU-120596. Thus, different type I PAMs increase open-channel lifetime and induce episodes of sustained activation of human α7 through different binding sites. Nevertheless, it is important to note that our results cannot discard that 5-HI may bind either to the PNU-120596 site but interact with different residues within the cavity, or to a partial overlapping site. Therefore, until the location of the binding site(s) is defined, it is cautious to refer to different structural determinants between PNU-120596 and 5-HI potentiation.

Overall, this study provide novel information regarding human α7 potentiation at the single-channel level, which emerges as a key requisite for the evaluation of potential clinical applications of PAMs.

5. CONCLUSIONS

Decline of α7 has been implicated in various neurological diseases, such as schizophrenia and Alzheimer's disease. Positive allosteric modulators (PAMs) are emerging as promising therapeutic strategies for these disorders. PAMs have been classified on the basis of their macroscopic effects as type I, which enhance peak currents, or type II, which also delay desensitization and reactivate desensitized receptors. The microscopic origin of these macroscopic profiles remains unclear for most PAMs. Considering the wide spectrum of potential clinical uses of PAMs, understanding the underlying molecular mechanism of potentiation at human α7 is urgent. In this study, we used high-resolution single-channel recordings to compare the actions of prototypic type I and type II PAMs as well as other less characterized PAMs, which macroscopically behave as type II PAMs. Our study reveals that all

PAMs enhance, although to a different extent, open-channel lifetime and activation episodes. This indicates that also type I PAMs affect α7 activation kinetics. By using a mutant α7 receptor that is insensitive to the prototype type II PAM (PNU-120596), we show that some though not all type I PAMs share structural determinants required for potentiation with type II PAMs. Because clinical and preclinical studies take place at a physiological temperature we also evaluated single-channel activity at this temperature. We found that the different PAM types show different sensitivity to temperature, suggesting different mechanisms of potentiation. A thorough molecular knowledge of α7 potentiation is required for the still ongoing development of therapeutic compounds.

ACKNOWLEDGMENTS

This work was supported by grant from Universidad Nacional del Sur (UNS), Consejo Nacional de Investigaciones Científicas y Técnicas (CONICET), and FONCYT [to CB], and from the Polish National Science Center (Sonata funding, UMO-2013/09/D/NZ7/04549) [to H.R.A. (Co-PI)]. We thank Dr. C. daCosta and Dr. Sine for providing mutants.

REFERENCES

Albuquerque EX, Pereira EF, Alkondon M, Rogers SW (2009) Mammalian nicotinic acetylcholine receptors: from structure to function. Physiol Rev 89:73-120.

Andersen N, Corradi J, Bartos M, Sine SM, Bouzat C (2011) Functional relationships between agonist binding sites and coupling regions of homomeric Cys-loop receptors. J Neurosci 31:3662-3669.

Andersen N, Corradi J, Sine SM, Bouzat C (2013) Stoichiometry for activation of neuronal alpha7 nicotinic receptors. Proc Natl Acad Sci U S A 110:20819-20824.

Arias HR (2010) Positive and negative modulation of nicotinic receptors. Adv Protein Chem Struct Biol 80:153-203.

Arias HR, Gu RX, Feuerbach D, Guo BB, Ye Y, Wei DQ (2011) Novel positive allosteric modulators of the human alpha7 nicotinic acetylcholine receptor. Biochemistry 50:5263-5278.

Arias HR, Targowska-Duda KM, Feuerbach D, Jozwiak K (2015) The antidepressant-like activity of nicotine, but not of 3-furan-2-yl-N-p-tolyl-acrilamide, is regulated by the nicotinic receptor β4 subunit.

Bagdas D, Targowska-Duda KM, Lopez JJ, Perez EG, Arias HR, Damaj MI (2015) The Antinociceptive and Antiinflammatory Properties of 3-furan-2-yl-N-p-tolyl-acrylamide, a Positive Allosteric Modulator of alpha7 Nicotinic Acetylcholine Receptors in Mice. Anesth Analg 121:1369-1377.

Bertrand D, Gopalakrishnan M (2007) Allosteric modulation of nicotinic acetylcholine receptors. Biochem Pharmacol 74:1155-1163.

Bertrand D, Bertrand S, Cassar S, Gubbins E, Li J, Gopalakrishnan M (2008) Positive allosteric modulation of the alpha7 nicotinic acetylcholine receptor: ligand interactions with distinct binding sites and evidence for a prominent role of the M2-M3 segment. Mol Pharmacol 74:1407-1416.

Bouzat C, Bren N, Sine SM (1994) Structural basis of the different gating kinetics of fetal and adult acetylcholine receptors. Neuron 13:1395-1402.

Bouzat C, Gumilar F, Spitzmaul G, Wang HL, Rayes D, Hansen SB, Taylor P, Sine SM (2004) Coupling of agonist binding to channel gating in an ACh-binding protein linked to an ion channel. Nature 430:896-900.

Bouzat C, Bartos M, Corradi J, Sine SM (2008) The interface between extracellular and transmembrane domains of homomeric Cys-loop receptors governs open-channel lifetime and rate of desensitization. J Neurosci 28:7808-7819.

Chatzidaki A, Millar NS (2015) Allosteric modulation of nicotinic acetylcholine receptors. Biochem Pharmacol.

Chatzidaki A, D'Oyley JM, Gill-Thind JK, Sheppard TD, Millar NS (2015) The influence of allosteric modulators and transmembrane mutations on desensitisation and activation of alpha7 nicotinic acetylcholine receptors. Neuropharmacology 97:75-85.

Collins T, Young GT, Millar NS (2011) Competitive binding at a nicotinic receptor transmembrane site of two alpha7-selective positive allosteric modulators with differing effects on agonist-evoked desensitization. Neuropharmacology 61:1306-1313.

Corradi J, Gumilar F, Bouzat C (2009) Single-channel kinetic analysis for activation and desensitization of homomeric 5-HT(3)A receptors. Biophys J 97:1335-1345.

daCosta CJ, Free CR, Corradi J, Bouzat C, Sine SM (2011) Single-channel and structural foundations of neuronal alpha7 acetylcholine receptor potentiation. J Neurosci 31:13870-13879.

daCosta CJ, Sine SM (2013) Stoichiometry for drug potentiation of a pentameric ion channel. Proc Natl Acad Sci U S A 110:6595-6600.

daCosta CJ, Free CR, Sine SM (2015) Stoichiometry for alpha-bungarotoxin block of alpha7 acetylcholine receptors. Nat Commun 6:8057.

Dani JA, Bertrand D (2007) Nicotinic acetylcholine receptors and nicotinic cholinergic mechanisms of the central nervous system. Annu Rev Pharmacol Toxicol 47:699-729.

Dilger JP, Brett RS, Poppers DM, Liu Y (1991) The temperature dependence of some kinetic and conductance properties of acetylcholine receptor channels. Biochim Biophys Acta 1063:253-258.

Dineley KT, Pandya AA, Yakel JL (2015) Nicotinic ACh receptors as therapeutic targets in CNS disorders. Trends Pharmacol Sci 36:96-108.

Dinklo T, Shaban H, Thuring JW, Lavreysen H, Stevens KE, Zheng L, Mackie C, Grantham C, Vandenberk I, Meulders G, Peeters L, Verachtert H, De PE, Lesage AS (2011) Characterization of 2-[[4-fluoro-3-(trifluoromethyl)phenyl]amino]-4-(4-pyridinyl)-5-thiazolemethanol (JNJ-1930942), a novel positive allosteric modulator of the {alpha}7 nicotinic acetylcholine receptor. J Pharmacol Exp Ther 336:560-574.

Dunlop J, Lock T, Jow B, Sitzia F, Grauer S, Jow F, Kramer A, Bowlby MR, Randall A, Kowal D, Gilbert A, Comery TA, Larocque J, Soloveva V, Brown J, Roncarati R (2009) Old and new pharmacology: positive allosteric modulation of the alpha7 nicotinic acetylcholine receptor by the 5-hydroxytryptamine(2B/C) receptor antagonist SB-206553 (3,5-dihydro-5-methyl-N-3-pyridinylbenzo[1,2-b:4,5-b']di pyrrole-1(2H)-carboxamide). J Pharmacol Exp Ther 328:766-776.

Fan H, Gu R, Wei D (2015) The alpha7 nAChR selective agonists as drug candidates for Alzheimer's disease. Adv Exp Med Biol 827:353-365.

Freedman R (2014) alpha7-nicotinic acetylcholine receptor agonists for cognitive enhancement in schizophrenia. Annu Rev Med 65:245-261.

Gill JK, Savolainen M, Young GT, Zwart R, Sher E, Millar NS (2011) Agonist activation of alpha7 nicotinic acetylcholine receptors via an allosteric transmembrane site. Proc Natl Acad Sci U S A 108:5867-5872.

Gronlien JH, Ween H, Thorin-Hagene K, Cassar S, Li J, Briggs CA, Gopalakrishnan M, Malysz J (2010) Importance of M2-M3 loop in governing properties of genistein at the alpha7 nicotinic acetylcholine receptor inferred from alpha7/5-HT3A chimera. Eur J Pharmacol 647:37-47.

Guerra-Alvarez M, Moreno-Ortega AJ, Navarro E, Fernandez-Morales JC, Egea J, Lopez MG, Cano-Abad MF (2015) Positive allosteric modulation of alpha-7 nicotinic receptors promotes cell death by inducing Ca(2+) release from the endoplasmic reticulum. J Neurochem 133:309-319.

Gumilar F, Bouzat C (2008) Tricyclic antidepressants inhibit homomeric Cys-loop receptors by acting at different conformational states. Eur J Pharmacol 584:30-39.

Gupta S, Auerbach A (2011) Temperature dependence of acetylcholine receptor channels activated by different agonists. Biophys J 100:895-903.

Hu M, Gopalakrishnan M, Li J (2009) Positive allosteric modulation of alpha7 neuronal nicotinic acetylcholine receptors: lack of cytotoxicity in PC12 cells and rat primary cortical neurons. Br J Pharmacol 158:1857-1864.

Hu XQ, Lovinger DM (2008) The L293 residue in transmembrane domain 2 of the 5-HT3A receptor is a molecular determinant of allosteric modulation by 5-hydroxyindole. Neuropharmacology 54:1153-1165.

Hurst R, Rollema H, Bertrand D (2013) Nicotinic acetylcholine receptors: from basic science to therapeutics. Pharmacol Ther 137:22-54.

Hurst RS, Hajos M, Raggenbass M, Wall TM, Higdon NR, Lawson JA, Rutherford-Root KL, Berkenpas MB, Hoffmann WE, Piotrowski DW, Groppi VE, Allaman G, Ogier R, Bertrand S, Bertrand D, Arneric SP (2005) A novel positive allosteric modulator of the alpha7 neuronal nicotinic acetylcholine receptor: in vitro and in vivo characterization. J Neurosci 25:4396-4405.

Jindrichova M, Lansdell SJ, Millar NS (2012) Changes in temperature have opposing effects on current amplitude in alpha7 and alpha4beta2 nicotinic acetylcholine receptors. PLoS ONE 7:e32073.

Kalappa BI, Sun F, Johnson SR, Jin K, Uteshev VV (2013) A positive allosteric modulator of alpha7 nAChRs augments neuroprotective effects of endogenous nicotinic agonists in cerebral ischaemia. Br J Pharmacol 169:1862-1878.

Lovinger DM, Sikes S, Zhou Q (2002) Rapid Drug Superfusion and Kinetic Analysis. In: Methods in Alcohol-Related Neuroscience Research (Liu Y, Lovinger DM, eds), pp 159-187. Boca Raton, Florida: CRC Press.

Malysz J, Gronlien JH, Anderson DJ, Hakerud M, Thorin-Hagene K, Ween H, Wetterstrand C, Briggs CA, Faghih R, Bunnelle WH, Gopalakrishnan M (2009) In vitro pharmacological characterization of a novel allosteric modulator of alpha 7 neuronal acetylcholine receptor, 4-(5-(4-chlorophenyl)-2-methyl-3-propionyl-1H-pyrrol-1-yl)benzenesulfonamide (A-867744), exhibiting unique pharmacological profile. J Pharmacol Exp Ther 330:257-267.

Ng HJ, Whittemore ER, Tran MB, Hogenkamp DJ, Broide RS, Johnstone TB, Zheng L, Stevens KE, Gee KW (2007) Nootropic alpha7 nicotinic receptor allosteric modulator derived from GABAA receptor modulators. Proc Natl Acad Sci U S A 104:8059-8064.

Palczynska MM, Jindrichova M, Gibb AJ, Millar NS (2012) Activation of alpha7 nicotinic receptors by orthosteric and allosteric agonists: influence on single-channel kinetics and conductance. Mol Pharmacol 82:910-917.

Papke RL, Porter Papke JK (2002) Comparative pharmacology of rat and human alpha7 nAChR conducted with net charge analysis. Br J Pharmacol 137:49-61.

Placzek AN, Grassi F, Papke T, Meyer EM, Papke RL (2004) A single point mutation confers properties of the muscle-type nicotinic acetylcholine receptor to homomeric alpha7 receptors. Mol Pharmacol 66:169-177.

Potasiewicz A, Kos T, Ravazzini F, Puia G, Arias HR, Popik P, Nikiforuk A (2015) Pro-cognitive activity in rats of 3-furan-2-yl-N-p-tolyl-acrylamide, a positive allosteric modulator of the alpha7 nicotinic acetylcholine receptor. Br J Pharmacol 172:5123-5135.

Rayes D, Spitzmaul G, Sine SM, Bouzat C (2005) Single-channel kinetic analysis of chimeric alpha7-5HT3A receptors. Mol Pharmacol 68:1475-1483.

Sahdeo S, Wallace T, Hirakawa R, Knoflach F, Bertrand D, Maag H, Misner D, Tombaugh GC, Santarelli L, Brameld K, Milla ME, Button DC (2014) Characterization of RO5126946, a Novel alpha7 nicotinic acetylcholine receptor-positive allosteric modulator. J Pharmacol Exp Ther 350:455-468.

Sitzia F, Brown JT, Randall AD, Dunlop J (2011) Voltage- and Temperature-Dependent Allosteric Modulation of alpha7 Nicotinic Receptors by PNU120596. Front Pharmacol 2:81.

Spurny R, Debaveye S, Farinha A, Veys K, Vos AM, Gossas T, Atack J, Bertrand S, Bertrand D, Danielson UH, Tresadern G, Ulens C (2015) Molecular blueprint of allosteric binding sites in a homologue of the agonist-binding domain of the alpha7 nicotinic acetylcholine receptor. Proc Natl Acad Sci U S A 112:E2543-E2552.

Sun YG, Pita-Almenar JD, Wu CS, Renger JJ, Uebele VN, Lu HC, Beierlein M (2013) Biphasic cholinergic synaptic transmission controls action potential activity in thalamic reticular nucleus neurons. J Neurosci 33:2048-2059.

Szabo AK, Pesti K, Mike A, Vizi ES (2014) Mode of action of the positive modulator PNU-120596 on alpha7 nicotinic acetylcholine receptors. Neuropharmacology 81:42-54.

Targowska-Duda KM, Feuerbach D, Biala G, Jozwiak K, Arias HR (2014) Antidepressant activity in mice elicited by 3-furan-2-yl-N-p-tolyl-acrylamide, a positive allosteric modulator of the alpha7 nicotinic acetylcholine receptor. Neurosci Lett 569:126-130.

Thomsen MS, Hansen HH, Timmerman DB, Mikkelsen JD (2010) Cognitive improvement by activation of alpha7 nicotinic acetylcholine receptors: from animal models to human pathophysiology. Curr Pharm Des 16:323-343.

Thomsen MS, El-Sayed M, Mikkelsen JD (2011) Differential immediate and sustained memory enhancing effects of alpha7 nicotinic receptor agonists and allosteric modulators in rats. PLoS ONE 6:e27014.

Timmermann DB, Gronlien JH, Kohlhaas KL, Nielsen EO, Dam E, Jorgensen TD, Ahring PK, Peters D, Holst D, Christensen JK, Malysz J, Briggs CA, Gopalakrishnan M, Olsen GM (2007) An allosteric modulator of the alpha7 nicotinic acetylcholine receptor possessing cognition-enhancing properties in vivo. J Pharmacol Exp Ther 323:294-307.

Uteshev V (2015) Are positive allosteric modulators of alpha7 nAChRs clinically safe? J Neurochem.

Uteshev VV (2014) The therapeutic promise of positive allosteric modulation of nicotinic receptors. Eur J Pharmacol 727:181-185.

Wallace TL, Porter RH (2011) Targeting the nicotinic alpha7 acetylcholine receptor to enhance cognition in disease. Biochem Pharmacol 82:891-903.

Wallace TL, Bertrand D (2013) Alpha7 neuronal nicotinic receptors as a drug target in schizophrenia. Expert Opin Ther Targets 17:139-155.

Williams DK, Wang J, Papke RL (2011a) Positive allosteric modulators as an approach to nicotinic acetylcholine receptor-targeted therapeutics: advantages and limitations. Biochem Pharmacol 82:915-930.

Williams DK, Wang J, Papke RL (2011b) Investigation of the molecular mechanism of the alpha7 nicotinic acetylcholine receptor positive allosteric modulator PNU-120596 provides evidence for two distinct desensitized states. Mol Pharmacol 80:1013-1032.

Williams DK, Peng C, Kimbrell MR, Papke RL (2012) Intrinsically low open probability of alpha7 nicotinic acetylcholine receptors can be overcome by positive allosteric modulation and serum factors leading to the generation of excitotoxic currents at physiological temperatures. Mol Pharmacol 82:746-759.

Yan H, Pan N, Xue F, Zheng Y, Li C, Chang Y, Xu Z, Yang H, Zhang J (2015) The coupling interface and pore domain codetermine the single-channel activity of the alpha7 nicotinic receptor. Neuropharmacology 95:448-458.

Yang JS, Seo SW, Jang S, Jung GY, Kim S (2012) Rational engineering of enzyme allosteric regulation through sequence evolution analysis. PLoS Comput Biol 8:e1002612.

Young GT, Zwart R, Walker AS, Sher E, Millar NS (2008) Potentiation of alpha7 nicotinic acetylcholine receptors via an allosteric transmembrane site. Proc Natl Acad Sci U S A 105:14686-14691.

Zhou Q, Verdoorn TA, Lovinger DM (1998) Alcohols potentiate the function of 5-HT3 receptor-channels on NCB-20 neuroblastoma cells by favouring and stabilizing the open channel state. J Physiol 507 (Pt 2):335-352.

Zwart R, De FG, Broad LM, McPhie GI, Pearson KH, Baldwinson T, Sher E (2002) 5-Hydroxyindole potentiates human alpha 7 nicotinic receptor-mediated responses and enhances acetylcholine-induced glutamate release in cerebellar slices. Neuropharmacology 43:374-384.

NEUROPHARM-D-15-00906
Andersen et al.

Highlights

- Potentiation of α7 is analyzed at the single-channel level.
- Type I and II PAMs prolong open-channel lifetime and activation episodes.
- Temperature sensitivity and structural determinants differ between PAM types.
- Some though not all type I PAMs share structural determinants of type II PAMs.